J Mater Sci (2007) 42:2261–2266
DOI 10.1007/s10853-006-0549-y

4TH BRAZILIAN MRS MEETING

Effects of hydrogen on the mechanical properties of a 2 1/4Cr–1Mo steel

P. C. Siquara · C. B. Eckstein · L. H. de Almeida · D. S. dos Santos

Received: 4 November 2005 / Accepted: 8 June 2006 / Published online: 13 March 2007

Abstract This paper explores the effects of hydrogen on the mechanical properties of a 2 1/4Cr–1Mo steel. The results for both microstructural conditions, as received and aged, indicated a loss of ductility after hydrogen charging treatment, but the yield strength and ultimate tensile strength remained unaltered. The fractograph analysis revealed that the fracture mode was modified by the hydrogen. The steel in the as-received condition showed craters and fisheyes on the fracture surface. The aged steel showed a brittle appearance associated with cleavage facets and small portion of areas with dimples. The hydrogen diffusivity and solubility were investigated using electrochemical permeation technique. It was observed that the hydrogen diffusivity decreased from $2.3 \pm 0.4 \times 10^{-10}$ m^2 s^{-1} in the as-received condition to $5.7 \pm 0.1 \times 10^{-11}$ m^2 s^{-1} in the aged condition. The hydrogen solubility showed an increase for the aged condition in comparison to the as received sample. Both phenomena can be attributed to carbide evolution during aging, resulting in an increase of the carbide/matrix interfacial area.

P. C. Siquara (✉) · L. H. de Almeida · D. S. dos Santos
PEMM – COPPE/UFRJ, P.O. Box 68505, 21941-972 Rio de Janeiro, RJ, Brazil
e-mail: psiquara@metalmat.ufrj.br

C. B. Eckstein
CENPES-Petrobras, Cidade Universitária, Rio de Janeiro, RJ, Brazil

Introduction

In petrochemical and petroleum refining industries, hydrogenation technologies, such as hydro-desulfurizing, hydrofining and hydro-cracking are used extensively, operating at elevated temperatures and pressures. Hydrogenation reactors are generally constructed using low alloy Cr–Mo ferritic steels, such as 2 1/4Cr–1Mo steel. These alloys are used because they possess excellent strength, toughness, low thermal expansion coefficient and corrosion resistance relative to carbon steels and most low alloy steels [1]. Also the Cr–Mo alloys have good resistance to hydrogen attack as indicated in API 941 [2]. This steel operates generally at pressures near of 20 MPa and temperatures in the range of 350 to 475 °C. During service these pressure vessel steels, especially 2 1/4Cr–1Mo steel, are susceptible to temper and/or hydrogen embrittlement [3].

Temper embrittlement (TE) is a phenomenon that occurs above room temperature when alloy steels are held within, or are cooled slowly through, an embrittling temperature range of 370–555 °C. TE is manifested by the increase of the ductile-to-brittle transition temperature, the fracture paths following prior austenitic grain boundaries [4].

Hydrogen embrittlement occurs in general at temperatures below 200 °C during shutdown operation. Because hydrogen is soluble in Cr–Mo alloy steels, atomic hydrogen diffuses into the reactor wall during operation at elevated temperatures [4]. In the temperature range of 300–500 °C, other degradation phenomena can occur such as hydrogen attack. The dissolved hydrogen diffuses into steel and reacts with the carbon in solid solution or with carbides to form methane [4].

Although the atomic volume of hydrogen dissolved in α-Fe is small, its influence is significant. Hydrogen migrates into the regions of the crystal lattice where stress concentration exists due to metallurgical defects such as precipitates, second phases and interfaces which result in embrittlement of the alloy. This can occur rapidly at room temperature in the bcc structure because of the high diffusivity of hydrogen in α-iron. In fact, the presence of hydrogen in the steel reduces tensile and toughness properties often resulting in catastrophic consequences. These problems have increased the need to understand and quantify the effects of hydrogen migration in steel by, for example, electrochemical hydrogen permeation tests.

The aim of this work is to characterize changes in the mechanical properties of a 2 1/4Cr–1Mo steel used in hydrogenation reactors in the as-received condition and aged in service at high temperature.

Experimental procedure

The steel used in this investigation was a 2 1/4Cr–1Mo ferritic steel (ASTM 387, Gr 22) obtained from 12 mm and 50 mm thick plates in the as-received condition and aged in service for 219,000 h at 550 °C, respectively. The chemical composition of the steels used in this study is given in Table 1 [5].

An OLYMPUS BX60M optical microscope and JEOL JSM 6460LV scanning electron microscope were employed to observe the microstructures of the hydrogenated and not hydrogenated specimens. The metallographic specimens were etched with 2% nital reagent.

Replicas from each specimen were prepared and then examined in a JEOL-2010 FX transmission electron microscope (TEM).

In the hydrogen charging treatment the specimens were cathodically charged with hydrogen to achieve a saturated condition. At room temperature, the hydrogen charging was performed installing the specimen in an electrolytic cell with a solution of a 0.1 M H_2SO_4 + 2 mg As_2O_3 and applying a current density of 100 A m^{-2} for 72 h.

Cylindrical tensile test samples were machined to 6 mm diameter and 40 mm in length and tensile tests were performed at room temperature in an EMIC test machine. The specimens were loaded to breaking point at a constant strain rate of 2×10^{-5} s^{-1}. The fracture surfaces were analyzed in a JEOL JSM 6460LV scanning electron microscope.

Samples of approximately 0.8 mm in thickness were machined for electrochemical permeation tests at room temperature. These tests were undertaken using an electrochemical cell comprising of two compartments separated by the sample. In one of the compartments a constant cathodic current was applied to generate hydrogen at the surface of the metal foil, using a solution of 0.1 M H_2SO_4 + 2 mg As_2O_3 as electrolyte. In the other compartment a weak anodic potential was applied in order to maintain a zero hydrogen concentration at surface, using a solution of 0.1N NaOH. This anodic current was monitored until steady state conditions were achieved, the diffusion rate of hydrogen through the sample, hydrogen flux, was recorded as a function of time. For all samples, the value of cathodic current applied for hydrogen generation was 1 mA. The results were the average of at least three specimens for each test condition.

The evolution of the hydrogen flux (J_L) with time (t), exhibits a sigmoidal relationship. Assuming the diffusivity of hydrogen does not to vary with the concentration, this flux may be expressed as [6]:

$$J_L = I_\infty \left(1 - \frac{4}{\pi}\sum_{0}^{\omega}\frac{(-1)^n}{2n+1}\exp\left(\frac{-(2n+1)^2\pi^2 D_{\text{app}}(t)}{4L^2}\right)\right) \quad (1)$$

where J_∞ is the steady state flux, D_{app} is the apparent hydrogen diffusivity, L is the sample thickness and n is the term of series, which is $n = 1, 2, 3, \ldots$

The apparent hydrogen solubility, S_{app}, can be determined by the integration of hydrogen flux by applying the follow equation:

$$S_{\text{app}} = \frac{1}{L}\int_0^t J_L(t)\mathrm{d}t \quad (2)$$

The apparent hydrogen diffusivity can be determined by the follow equation [6]:

$$t_b = \frac{0.76L^2}{\pi^2 D_{\text{app}}} \quad (3)$$

Table 1 Chemical composition of the 2 1/4Cr–1Mo steels (wt%) used in this study

	C	Mn	P	S	Si	Cr	Mo
As-received	0.192	0.660	0.018	0.009	0.253	2.22	0.96
Aged	0.249	0.530	0.008	0.014	0.269	2.26	0.98

where t_b is the breakthrough time corresponding to the intercept of a tangent to the permeation curve with the time axis.

Results and discussion

Figures 1 and 2 show the bainitic microstructure of the as-received and aged steels. Grain growth and secondary precipitation can be observed in the aged condition compared with the as-received steel. A higher carbon content of the aged alloy contributes also for the increase of the carbide volume fraction. Preferential precipitation at grain boundaries can be also noted during secondary precipitation. Such morphological modifications are typical of long term operation at high temperatures in this steel. Carbide evolution during aging is widely reported in literature for 2 1/4Cr–1Mo steels [7, 8]. The primary carbides such as M_3C and M_7C_3 evolves to more stable ones such as $M_{23}C_6$ and M_6C. At the same time during aging M_2C precipitates at the expenses of Mo in solid solution as observed in the aged conditions studied in the present work. The as-received condition exhibited M_2C e M_7C_3 that are the typical carbides for the as-received condition and the aged condition exhibited $(MoCr)_2CN$, M_7C_3 e M_6C.

Table 2 shows the tensile tests results where σ_y, σ_u and ε are the yield stress, the ultimate tensile strength and the total strain, respectively. The effect of hydrogen on the mechanical properties is typified by the loss of ductility which may cause premature failure under static load. The ductility decreases from 21.5 ± 1.5% to 9.6 ± 2.9% for as-received steel and for the aged steel from 21.9 ± 0.9% to 7.9 ± 1.8%. The loss of ductility is directly correlated with the quantity of hydrogen in the steel, indicating that the aged steel had absorbed more hydrogen, as shown later. Moreover, steel with fine and spherical carbides is more resistant to hydrogen embrittlement than steel with coarser and more angular carbides, as present in the aged steel [9].

The yield stress and tensile strength of the aged steel are 40–50% lower than those for the as received steel, this reduction was caused by overaging [10] and grain growth due to exposure to high temperatures for a long period. The presence of the hydrogen didn't influence these values.

The curves obtained for as-received and hydrogenated specimens are shown in Fig. 3. The curves of steel in the as-received condition show the yield point phenomenon caused by the interaction of the interstitial atoms and dislocations [10]. The tensile behavior of

Table 2 Results from tensile tests

Material	σ_y (MPa)	σ_u (Mpa)	ε (%)
As received	477 ± 6.8	587 ± 5.7	21.5 ± 1.5
As received + hydrogenated	469 ± 8.4	574 ± 7.7	9.6 ± 2.9
Aged	320 ± 5.5	475 ± 2.6	21.9 ± 0.9
Aged + hydrogenated	335 ± 6.0	466 ± 2.1	7.9 ± 1.8

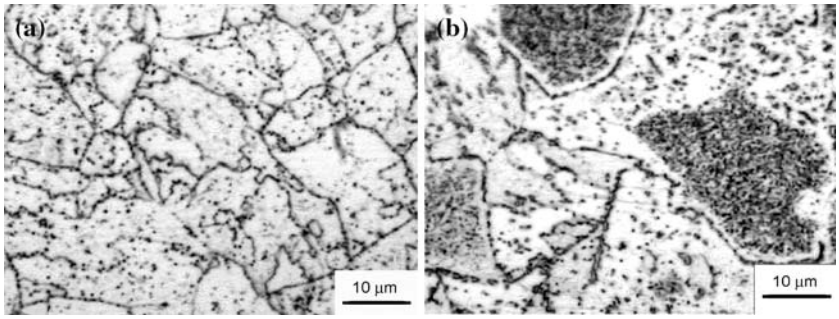

Fig. 1 Optical micrographs of the microstructure of 2 1/4Cr–1Mo steel (**a**) as received and (**b**) aged steels (1,000×)

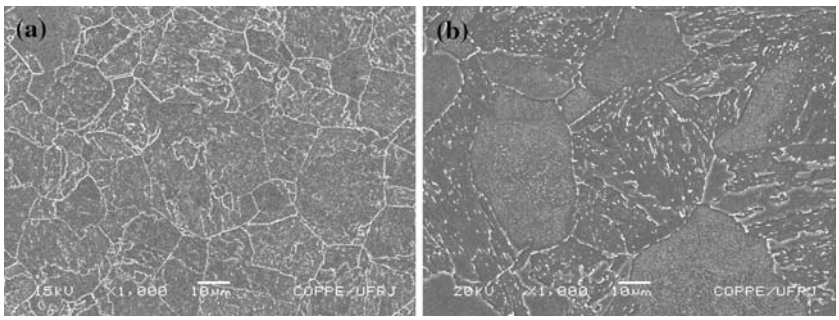

Fig. 2 SEM of the microstructure of 2 1/4Cr–1Mo steel (**a**) as received (1,000×) and (**b**) aged steels (1,000×)

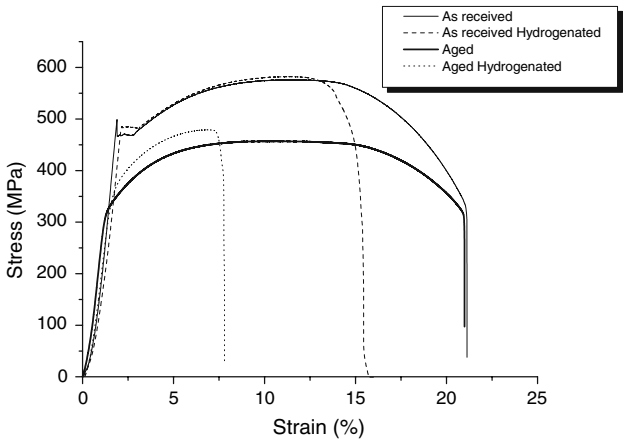

Fig. 3 Stress–strain plot at room temperature for 2 1/4Cr–1Mo steel samples with hydrogen and without hydrogen

the aged steel indicates that the steel was relatively ductile. The fracture occurred by microvoid coalescence and considerable necking was observed (Fig. 4a). The characteristic cup and cone appearance was observed and the fracture surface showed dimples (Fig. 4b). The same behavior was observed for the as-received steel.

A decrease in the strain to failure was observed for the hydrogen charged specimens. It is worth to noting that, in the presence of hydrogen, a slight strengthening of the steel occurred. As a rule, the fracture of all hydrogen charged specimens was mainly brittle. Figure 5 shows the fracture surface of the as-received steel charged with hydrogen. The appearance of the fracture is completely modified by the action of the hydrogen. Circular craters are visible (Fig. 5a). The accumulation of hydrogen around the inclusions affects the void nucleation caused by internal hydrogen gas pressurization and hydrogen-induced reduction in critical interfacial strength. During loading, the hydrogen released by the interfaces can cause internal cracks around inclusions to grow in a brittle manner resulting in fisheyes on fracture surface [2, 11, 12]. Figure 5b shows a fisheye, an inclusion can be noted in the center of the crater. Cleavage facets appear radially surrounding the non-metallic inclusion revealing the characteristic of drastic brittleness of this portion of material. The presence of craters in this steel can be attributed to the fact that the occurrence of fisheye cracks increases with decreasing volume fraction and carbide particle size [13].

Strnadel [11] has developed a model to predict fisheye crack size at the fracture surface as a function of temperature [11]. He has assumed that the initiation of microcracks is caused by a local increase in hydrogen concentration at inclusions. The propagation at these microcracks results in fisheye formation and is controlled by the local stress intensity factor and fracture resistance of the matrix.

For the aged steel, the behavior of the fracture was different. Hydrogen damage is evident and is revealed in the fractographs (Fig. 6), as indicated by the brittle appearance (Fig. 6a) and cleavage facets with a small portion of dimples (Fig. 6b).

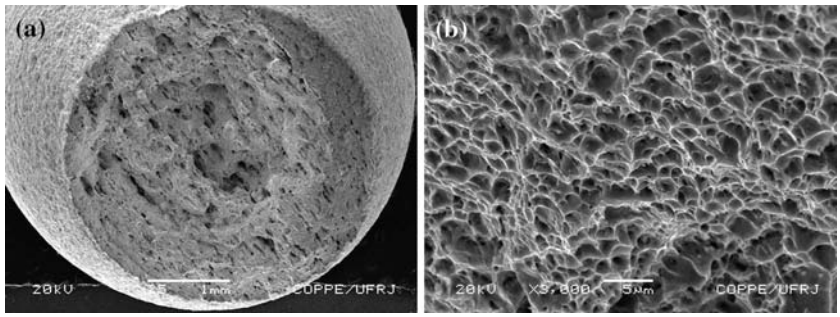

Fig.4 SEM fractographs of aged steel: (**a**) ductile fracture surface of the neck (25×) and (**b**) the dimples obtained (3,000×)

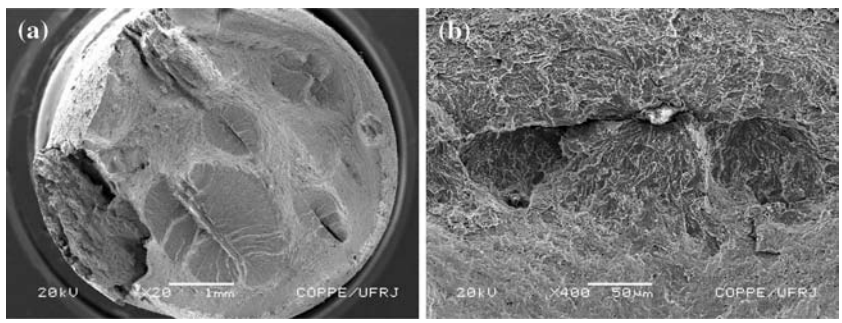

Fig. 5 SEM fractographs of the as received steel hydrogenated: (**a**) presence of craters (20×) and (**b**) a fisheye (400×)

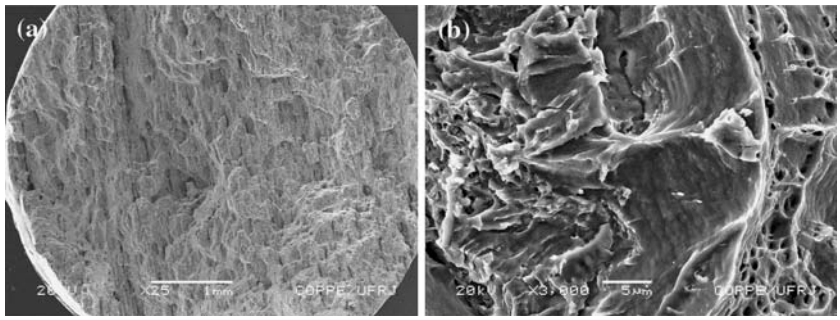

Fig. 6 SEM fractographs of aged steel hydrogenated: (**a**) brittle facets on the fracture surface (25×) and (**b**) appearance of cleavage(3,000×)

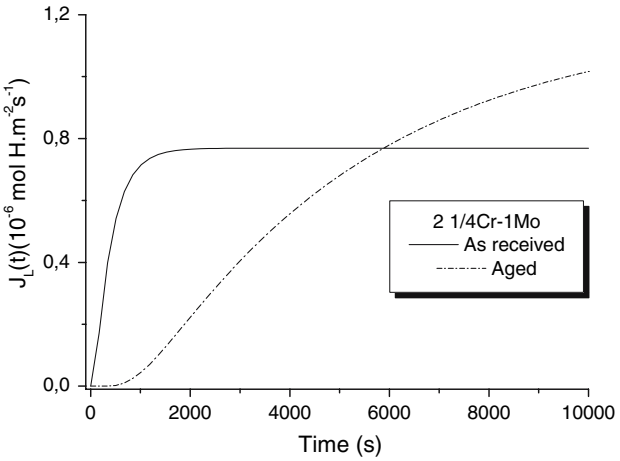

Fig. 7 Hydrogen permeation curves of the as received and aged steels

Table 3 Hydrogen parameters of steel at room temperature for cathodic charging equal to 1 mA

Sample	D_{app} (m^2 s^{-1})	S_{app} (mol H m^{-3})
As received	$2.0 \pm 0.4 \times 10^{-10}$	1.3 ± 0.5
Aged	$7.6 \pm 0.1 \times 10^{-11}$	11.7 ± 0.4

The hydrogen permeation curves are shown in Fig. 7. The hydrogen diffusivity (D_{app}) and apparent solubility (S_{app}) obtained from these curves are presented in Table 3 for as-received and aged specimens. It has been reported that the diffusivity of hydrogen in pure α-Fe is very high and is of the order of 10^{-9} m^2 s^{-1} [12]. The diffusivity in low alloy ferritic steel is about the same as that of α-Fe. However, the diffusivity of the as-received condition is lower by one order of magnitude. This is due to the presence of defects in the microstructure such as grain boundaries, dislocations or precipitate/matrix interfaces which are favorable sites for the trapping of hydrogen. At temperatures below about 200 °C diffusion is hindered by these traps which capture hydrogen and delay the diffusion [12]. The aged material showed high solubility and low diffusivity when compared to the as-received material. Furthermore, the time that the hydrogen took to cross the aged sample is longer than the time for the as-received sample.

Thus, the high value of the solubility for the aged steel is due to the presence of coalesced carbides, which are favorable sites for the trapping of hydrogen, according to the results of the autoradiographic work presented by Garet et al. [14].

Conclusions

The current work presents a comparison between the as-received and aged condition for a 2 1/4Cr–1Mo steel used in hydrogenation reactors. Hydrogen permeation and tensile tests shows that the hydrogen embrittlement susceptibility was affected by the microstructural condition of the sample. The aged steel contained a higher concentration of hydrogen than the as-received steel under the same cathodic charging conditions. The high solubility in the aged steel may be interpreted in terms of an increased capacity of hydrogen trapping caused by the presence of coarse and more stable carbides as well as a higher carbide volume fraction that, in turn, results in an increase of the interfacial area.

The influence of hydrogen on the mechanical properties of a 2 1/4Cr–1Mo steel after aging was investigated. The predominant effect of H on the properties of this steel is a decrease in ductility associated with the change in fracture mode from ductile shear rupture to brittle fracture.

Acknowledgment The authors acknowledge the financial support of CNPq, CAPES, FAPERJ and PETROBRAS for this work.

References

1. ASM (1990) Metals handbook, vol 1. Metals Park, Ohio
2. American Petroleum Institute (1998) Publication 941, Steels for hydrogen service at elevated temperatures and pressures in petroleum refineries and petrochemical plants, Supplement 1. Washington

3. Tan J, Chao YJ (2005) Mater Sci Eng A405:214
4. Antalffy LP, Chaku PN, Canonico DA, Pfeifer JA, Alcorn DG (2002) Int J Pressure Vessels Piping 79:561
5. ASTM A387/A 387M (1999) Standard specification for pressure vessels plates. Alloy Steel, Chromium-Molybdenum
6. Boes N, Zuchner H (1976) J Less-Common Met 49:223
7. Parvathavarthini N, Saroja S, Dayal RK, Khatak HS (2001) J Nuclear Mater 288:187
8. Tsai MC, Yang JR (2003) Mater Sci Eng A340:15
9. Timmins PF (1997) ASM international. Materials Park, Ohio
10. George ED (1961) Mechanical metallurgy. McGraw-Hill
11. Strnadel B (1998). Eng Fract Mech 61:299
12. Dayal RK, Parvathavarthini N (2003) Sadhana 28:431
13. Hang GW, Song YJ (1995) Scripta Metall Mater 32:1107
14. Garet M, Brass AM, Haut C, Guttierez-Solana F (1998) Corros Sci 40:1073